Hyperpolarization-Activated Current I_h Disconnects Somatic and Dendritic Spike Initiation Zones in Layer V Pyramidal Neurons

Thomas Berger, Walter Senn, and Hans-R. Lüscher
Institute of Physiology, University of Bern, CH-3012 Bern, Switzerland

Berger, Thomas, Walter Senn, and Hans-R. Lüscher. Hyperpolarization-activated current I_h disconnects somatic and dendritic spike initiation zones in layer V pyramidal neurons. *J Neurophysiol* 90: 2428–2437, 2003. First published June 11, 2003; 10.1152/jn.00377.2003. Layer V pyramidal cells of the somatosensory cortex operate with two spike initiation zones. Subthreshold depolarizations are strongly attenuated along the apical dendrite linking the somatic and distal dendritic spike initiation zones. Sodium action potentials, on the other hand, are actively back-propagating from the axon hillock into the apical tuft. There they can interact with local excitatory input leading to the generation of calcium action potentials. We investigated if and how back-propagating sodium action potentials alone, without concomitant excitatory dendritic input, can initiate calcium action potentials in the distal dendrite. In acute slices of the rat somatosensory cortex, layer V pyramidal cells were studied under current-clamp with simultaneous recordings from the soma and the apical dendrite. A train of four somatic action potentials had to reach high frequencies to induce calcium action potentials in the dendrite ("critical frequency," CF $\sim$100 Hz). Depolarization in the dendrite reduced the CF, while hyperpolarization increased it. The CF depended on the presence of the hyperpolarization-activated current I_h: blockade with 20 μM 4-(*N*-ethyl-*N*-phenylamino)-1,2-dimethyl-6-(methylamino) pyridinium chloride (ZD7288) reduced the CF to 68% of control. If the neurons were stimulated with noisy current injections, leading to in-vivo-like irregular spiking, no calcium action potentials were induced in the dendrite. However, after I_h channel blockade, calcium action potentials were frequently seen. These data suggest that I_h prevents initiation of the dendritic calcium action potential by proximal input alone. Dendritic calcium action potentials may therefore represent a unique signature for coincident somatic and dendritic activation.

INTRODUCTION

The layer V pyramidal cell of the somatosensory cortex can generate action potentials at two spatially separated locations (Larkum et al. 1999b; Schiller et al. 1997). A low-threshold sodium spike is initiated in the axon hillock, whereas a high-threshold calcium spike may be generated in the distal apical dendrite (at $\sim$550–900 μm distance from the soma) (Larkum and Zhu 2002). Sodium spikes are actively propagated on their way back into the dendrite due to the presence of voltage-gated sodium channels (Stuart and Sakmann 1994). The further the back-propagating action potential penetrates into the apical dendrite, the more active propagation properties are substituted by passive current spread. This leads to attenuation and broadening of the action potential and enables their temporal sum-

mation. Therefore the extent to which the dendritic action potentials can propagate depends also on the electrotonic properties of the dendrite. Back-propagating action potentials interact with dendritic synaptic potentials and can lead to long-lasting calcium action potentials which in turn initiate bursts of sodium action potentials in the axon hillock (back-propagation-activated calcium spike firing, BAC firing) (Larkum et al. 1999b). The resulting change in the output pattern of the cell from single spikes to bursts reflects the detection of simultaneous somatic and dendritic inputs.

The density of the hyperpolarization-activated current I_h (Kaupp and Seifert 2001; Pape 1996) is higher in the distal apical dendrite of layer V cells in comparison to the proximal region of the dendrite and the soma (Berger et al. 2001; Lörincz et al. 2002; Williams and Stuart 2000a). I_h leads to the attenuation of synaptic potentials and impairs their summation (Berger and Lüscher 2003; Berger et al. 2001; Williams and Stuart 2000a, 2002). In spite of the uneven distribution of this conductance, the apical dendrite of these cells behaves linearly in the subthreshold range (Berger et al. 2001) and the excitatory postsynaptic potential (EPSP) shape is primarily affected by the shunting effect of I_h. In addition, I_h may modulate the back-propagation of sodium action potentials and thereby their ability to initiate BAC firing.

Layer V pyramidal cells receive synaptic input from different sources through different layers. This property puts layer V pyramidal cells into the unique position to associate concomitant bottom-up input to the soma and the basal dendrites on one side and top-down inputs to the distal apical dendrite on the other side. Simultaneous activation of the two inputs leads to BAC firing resulting in a burst of action potentials (Larkum et al. 1999b). To enable this associative mechanism, a high density of voltage-gated sodium and calcium channels is needed in the dendrite. This actively supports the back-propagation of action potentials in the dendrite and the generation of calcium spikes. To differentiate this mechanism from normal cell firing, activation of the somatic spike initiation zone alone should not initiate dendritic calcium action potentials. Under these conditions, a long "electrotonic distance" between the two zones is essential. The presence of leak conductances mediated by potassium channels or I_h helps to disconnect both initiation zones in the subthreshold range (Berger et al. 2001). In the present work, we examined if I_h prevents the generation

---

Address for reprint requests and other correspondence: T. Berger, Institute of Physiology, University of Bern, Bühlplatz 5, CH-3012 Bern, Switzerland (E-mail: berger@pyl.unibe.ch).

of supra-threshold calcium events in the distal dendrite due to somatic spikes.

METHODS

Brain slice preparation and cell identification

Three-hundred-μm-thick parasagittal slices of the somatosensory cortex were prepared from 28- to 37-day-old Wistar rats according to national and institutional guidelines. Preparations were done in ice-cold extracellular solution using a vibratome (Microslicer DTK-1000, Dosaka, Kyoto, Japan). Slices were incubated at 37°C for 30 mins and then left at room temperature until recording. Layer V pyramidal neurons from the somatosensory area with a thick apical dendrite were visualized by infrared differential interference contrast videomicroscopy using a Newvicon camera (C2400, Hamamatsu, Hamamatsu City, Japan) and an infrared filter (RG9, Schott, Mainz, Germany) mounted on an upright microscope (Axioskop FS, Zeiss, Oberkochen, Germany).

Electrophysiology and intracellular stimuli

Current-clamp whole cell recordings were made either from the soma alone or simultaneously from the soma and apical dendrite of layer V pyramidal neurons. An Axoprobe-1A amplifier (Axon Instruments, Foster City, CA) was used. Resistance compensation and capacitance neutralization were applied. In-vivo-like input currents were generated as an Ornstein–Uhlenbeck process (Cox and Miller 1965). These noisy currents are Gaussian distributed with mean μ, standard deviation σ, and a correlation length τ, and follow the equation

$$I(t + dt) = I(t) + (\mu - I(t))dt/\tau + \sigma G_t \sqrt{2dt/\tau}$$

G_t is a Gaussian random variable with mean 0 and SD 1. Such a current mimics a large number of asynchronously firing excitatory and inhibitory presynaptic cells. These contribute to the mean μ and variance σ^2 according to $\mu = I_e r_e \tau + I_i r_i \tau$ and $\sigma^2 = I_e^2 r_e \tau/2 + I_i^2 r_i \tau/2$ (Tuckwell 1988). Here, $r_{e/i}$ represent the total firing rates of the presynaptic excitatory and inhibitory population, respectively, and $I_{e/i}$ are the peak amplitudes of a single excitatory and inhibitory postsynaptic current, respectively. These unitary currents are characterized by a sharp rise and an exponential decay with a time constant τ. The current amplitudes $I_{e/i}$ are the product of the peak conductance times the driving force, $I_{e/i} = g_e(E_{e/i} - V)$. A total mean and SD of $\mu = \sigma = 400$ pA, for instance, can be obtained with $r_e = 15,000$ Hz, $r_i = 8,000$ Hz, $g_e = 1$ nS, $g_i = 6$ nS, $E_e = 0$ mV, $E_i = -70$ mV, $\tau = 3$ ms, and a fixed membrane potential $V = -55$ mV. The total firing rates $r_{e/i}$ are the product of the number of synapses times the firing rate of the individual excitatory or inhibitory afferent fibers (e.g., 5,000 excitatory afferents each firing with a mean rate of 3 Hz, and 1,000 inhibitory afferents each firing with a mean rate of 8 Hz) (compare Abeles 1991; Schüz and Palm 1989).

Electrodes were made from borosilicate glass tubing (Hilgenberg, Malsfeld, Germany). The resistance was 4–6 MΩ for somatic and 10–16 MΩ for dendritic recording pipettes. All experiments were done at ~34°C. Data were low-pass filtered at 5 kHz using the internal filter of the amplifier. The sampling frequency was at least twice the filter frequency (10–20 kHz). Data were digitized and stored on-line using either Clampex8 (Axon Instruments) or a custom-made, Matlab-based acquisition and analysis program (www.cns.unibe.ch/MeeDuck). Data were analyzed off-line with Clampfit8 and Matlab. Pooled data are expressed as means ± SD.

Chemicals and solutions

Slices were continuously superfused with a physiological extracellular solution containing (in mM) 125 NaCl, 25 NaHCO$_3$, 2.5 KCl, 1.25 NaH$_2$PO$_4$, 2 CaCl$_2$, 1 MgCl$_2$, and 25 glucose, bubbled with 95% O$_2$-5% CO$_2$. Pipette solution contained (in mM) 110 K-gluconate, 30 KCl, 10 EGTA, 10 HEPES, 4 Mg-ATP, 0.3 Na$_2$-GTP, and 10 Na$_2$-Phosphocreatine, pH adjusted to 7.3 with KOH. The membrane potential values given were not corrected for the liquid junction potential. 4-(N-ethyl-N-phenylamino)-1,2-dimethyl-6-(methylamino) pyridinium chloride (ZD7288) was a generous gift from Astra-Zeneca (Macclesfield, UK). A stock of 50 mM ZD7288 was prepared in bidistilled water. Dilution in the extracellular solution provided the final concentration given in the Results section. All other drugs and chemicals were from Sigma or Merck.

RESULTS

To study the separation properties of I_h with regard to the two spike initiation zones, we performed three sets of experiments. First, simultaneous somatic and dendritic recordings were used to determine the critical frequency (CF) of back-propagating action potentials for eliciting a dendritic calcium action potential. In addition, the dependence of the CF from the dendritic membrane potential was investigated. Second, the CF was determined in the presence of a blocker of the hyperpolarization-activated current I_h. Third, the possibility of the cells to generate calcium action potentials was studied with in-vivo-like, noisy current injections.

Dendritic calcium spike initiation requires a high somatic action potential frequency

Is it possible to activate the distal dendritic calcium spike initiation zone in response to proximal synaptic input and the resulting somatic sodium action potentials? We used a well-defined stimulation paradigm previously developed by Larkum et al. (1999a). Four consecutive action potentials were induced at different frequencies in the soma of layer V pyramidal cells with short supra-threshold somatic current injections (3–5 nA for 2 ms; $V_m = -69.3 \pm 5.0$ mV, $R_{in} = 24.4 \pm 6.5$ MΩ, $n = 56$ cells; Fig. 1A). The spikes back-propagated into the dendrite. Above a CF of the back-propagating action potentials, a calcium-mediated action potential was elicited in the dendrite ($n = 22$ combined somato-dendritic recordings; distance of dendritic recording from the soma: 302 ± 92 μm). The presence of this dendritic calcium potential was also visible in the somatic recording as an additional afterdepolarization after the last spike (Figs. 1, A and B, 2A, and 3A). The calcium events were blocked by the combined bath application of 100 μM NiCl$_2$ and 200 μM CdCl$_2$ ($n = 5$ cells, Fig. 1B). This confirms the dependence of these events from the activation of voltage-gated calcium channels. Calcium action potentials were only present at high frequencies (CF = 104.5 ± 23.4 Hz; range: 55.5–166.7 Hz; $n = 56$ cells; Fig. 1D). The CF could also be defined using the integral below the voltage transient of the dendritic recording. This integral was plotted against the frequency of the somatic spikes (Fig. 1C), and it increased with frequency due to an improved temporal summation of the four dendritic action potentials. At the CF, a nonlinear increase reflected the activation of calcium conductances. With frequencies even higher than the CF, the integral decreased slightly. This could be explained by the relative refractory period of the sodium and calcium action potential at short inter-stimulus intervals (Fig. 1, A and C).

The CF was strongly modulated by the dendritic membrane potential. When four consecutive action potentials below the CF were combined with a depolarizing constant current injection
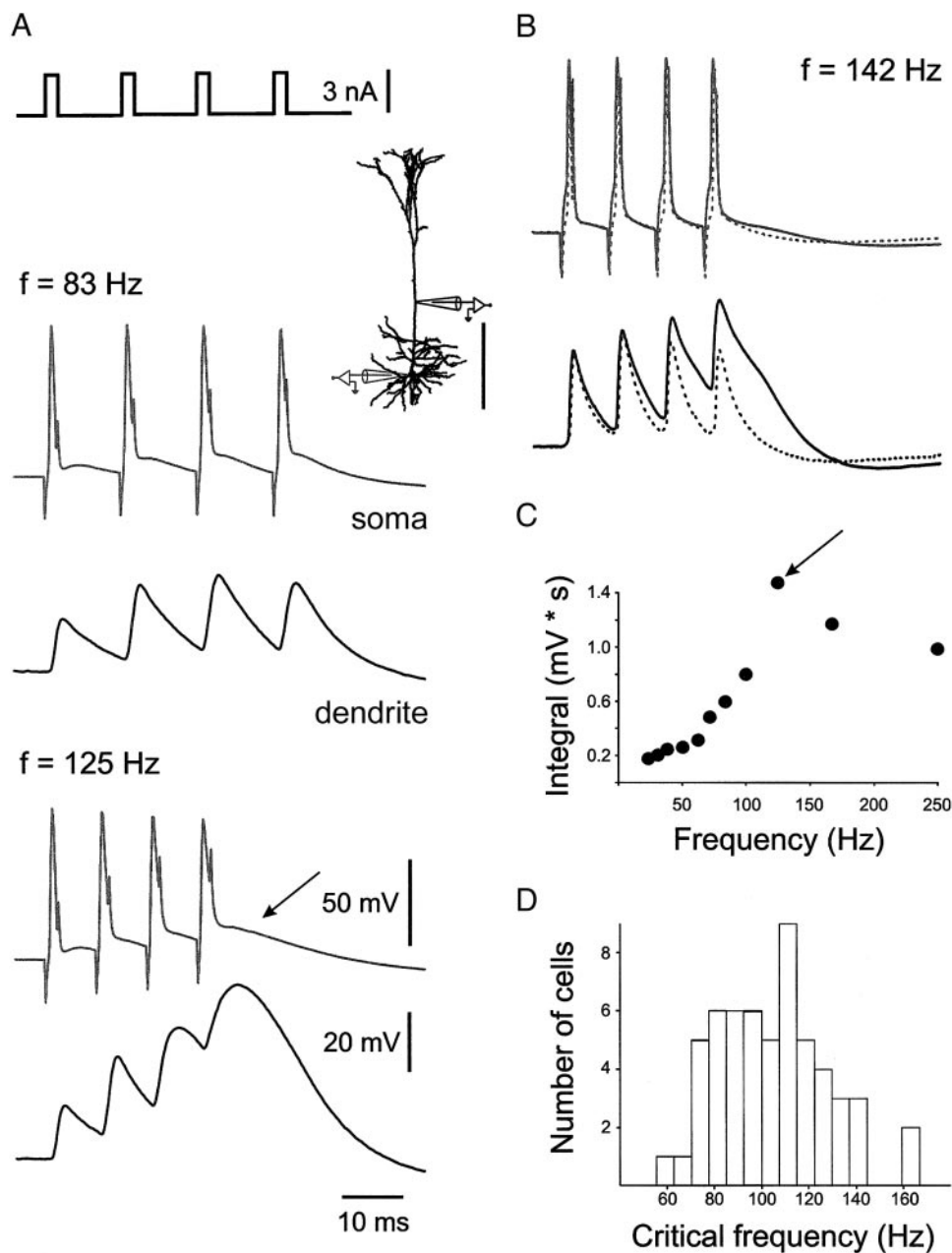
FIG. 1. Backpropagating action potentials can induce dendritic calcium potentials only beyond a high critical frequency. Simultaneous recording from the soma and the dendrite of a layer V pyramidal cell (see sketch in the *inset;* scale bar in the *inset*: 400 μm). In all figures, the *top traces* represent the somatic, the *bottom traces* the dendritic recordings. *A*: 4 consecutive action potentials are induced in the soma with short supra-threshold somatic current injections (pattern on top). The spikes are back-propagating into the dendrite and can evoke a dendritic calcium action potential depending on their frequency. The presence of this dendritic calcium potential is also visible in the somatic recording as an additional afterdepolarization following the last spike (see arrow. *B*: in another cell, combined bath application of 100 μM $NiCl_2$ and 200 μM $CdCl_2$ prevented the generation of the dendritic calcium action potential and of the somatic afterdepolarization (dotted traces). Same scale bars in *A* and *B*. *Rats P31* and *P35,* dendritic recordings 350 and 320 μm from the soma for *A* and *B,* respectively. *C*: the integral below the voltage transient of the dendritic recording reflecting the charge transferred is plotted against the frequency of the somatic spikes for the cell in *A*. A critical frequency (CF, arrow) of 125 Hz is obtained for the induction of a calcium spike. *D*: the CF from 52 cells is shown in a histogram.

into the dendrite, calcium action potentials were seen ($n = 3$ cells of 3; Fig. 2*A*). These changes in the ability to generate dendritic calcium action potentials reflected a decrease in the CF. Additional hyperpolarizing current injection into the dendrite did not change the shape of the somatic or dendritic recording significantly. Dendritic calcium events evoked beyond the CF could be prevented by the injection of a hyperpolarizing constant current (Fig. 2*B*), while depolarizing current increased their amplitude slightly. Dendritic hyperpolarization led to an increase in the CF. Thus combined somatic and excitatory dendritic activity decreased dramatically the amount of somatic activity necessary for dendritic calcium events.

I_h increases critical frequency

Application of the specific I_h blocker ZD7288 (20 μM) (Harris and Constanti 1995) reduces the CF to 68.2 $\pm$ 7.4% of control (78.4 $\pm$ 21.2 Hz; $P < 0.001$, paired *t*-test; $n = 11$ cells out of 11 tested; Fig. 3). To study the importance of neuromodulation of I_h via changes in the intracellular cAMP, we investigated the effect of different cAMP modulators. Bath application of serotonin (concentration range: 5–100 μM), isoproterenol (at concentrations of 1 and 10 μM), or dopamine (50 μM) did not influence the CF ($n = 12$ cells in total; not shown).

Blockade of I_h resulted in marked changes of the action potential shape in the dendrite and a larger afterdepolarization in the soma. In four of five somatodendritic recordings, application of 20 μM ZD7288 reduced the amplitude of the first dendritic action potential (Fig. 4*C*). However, the action potential amplitude was not significantly changed over all cells (69.9 $\pm$ 36.5% of the control value; control: 23.0 $\pm$ 6.2 mV; in ZD7288: 15.9 $\pm$ 8.0 mV; $n = 5$ cells; Fig. 4). The decay of
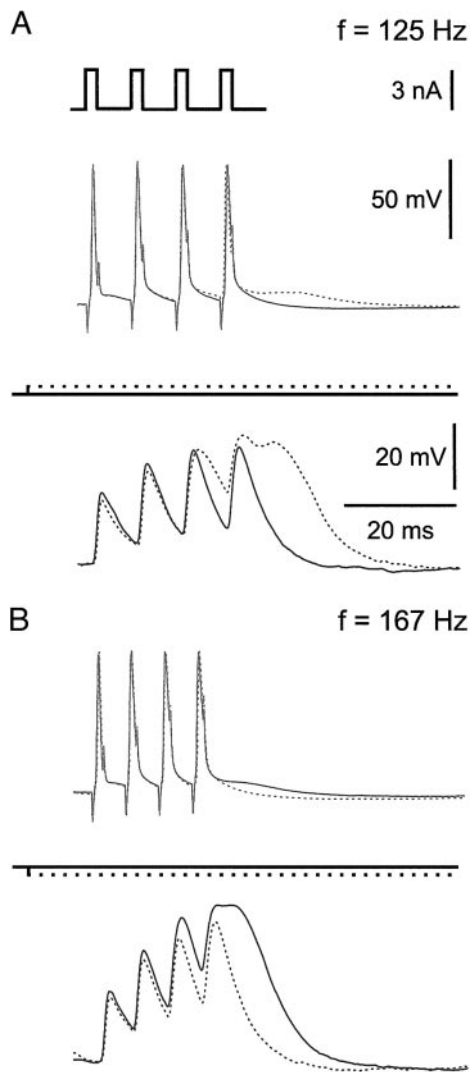
FIG. 2. Dendritic depolarization decreases, dendritic hyperpolarization increases the critical frequency. *A*: 4 consecutive action potentials with a spike frequency of 125 Hz cannot evoke calcium action potentials in the dendrite of this cell (continuous traces). If in addition to the generation of somatic spikes a depolarizing current (+250 pA) was injected into the dendrite, calcium action potentials were seen (dotted traces). *B*: in the same cell, 4 spikes with a frequency of 167 Hz resulted in a calcium action potential (continuous traces). Injection of a hyperpolarizing current (−250 pA) prevented these dendritic potentials (dotted traces). Same scale bars in *A* and *B*. Rat P33, dendritic recording 300 μm from the soma.

addition, the longer depolarization may have facilitated the activation of voltage-gated calcium channels underlying the calcium action potential. In turn, the somatic spike without I_h was characterized by a reduced fast afterhyperpolarization and an enlarged afterdepolarization, while rise and decay were only minimally affected (Fig. 4*C*). The afterdepolarization became larger from the first to the fourth spike and this increase may be due to the longer and larger forward-propagated dendritic action potentials.
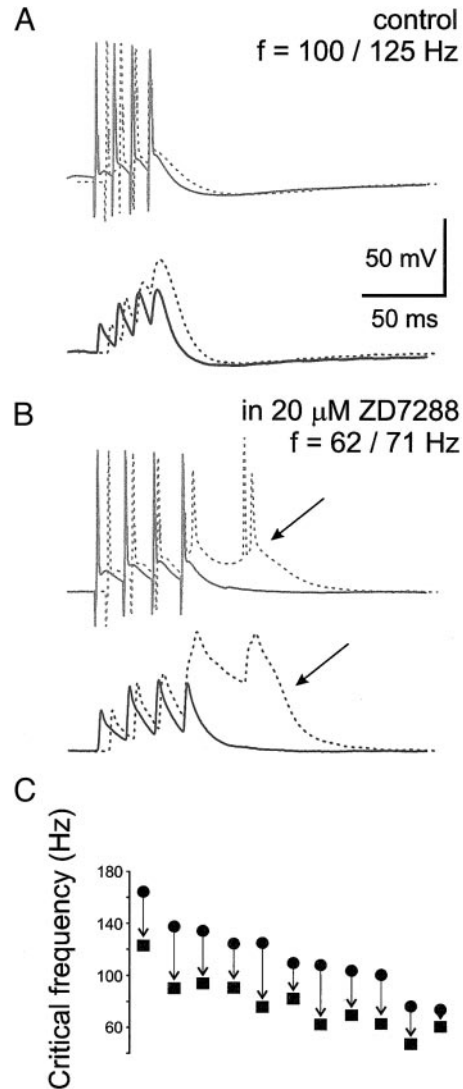

FIG. 3. High CF is due to the presence of I_h. *A*: using the same experimental paradigm as in Fig. 1, a critical frequency of 125 Hz for the induction of dendritic calcium potentials is found in this cell. Somatic and dendritic recordings are aligned to the beginning of the 4th spike and are shown superimposed. Four action potentials are induced at (dotted traces) and below (continuous traces) the CF. *B*: application of 20 μM 4-(*N*-ethyl-*N*-phenylamino)-1,2-dimethyl-6-(methylamino) pyridinium chloride (ZD7288), a specific blocker of the hyperpolarization-activated current I_h, results in a reduction of the CF to 7 Hz. Beyond the CF, additional somatic action potentials and concomitant dendritic calcium events can be seen (see arrows). Rat P33, dendritic recording 420 μm from the soma. *C*: for eleven cells, this shift in the CF due to block of I_h is shown (circles, control values of CF; rectangles, CF in 20 μM ZD7288).

the first dendritic action potential was fitted with a monoexponential function, yielding a decay time constant of 3.5 ± 1.2 ms under control conditions. Blocking I_h prolonged the dendritic action potential decay to values between 148 and 570% of control. The decay time of the calcium action potential could also be fitted with a monoexponential function (decay time constant under control: 5.9 ± 0.8 ms; under ZD7288: 10.0 ± 2.8 ms; $172.5 \pm 52.0\%$ of control; Fig. 4). This shortening of the dendritic calcium action potential with I_h was due to two factors: a change in the membrane time constant and the presence of an undershoot (Fig. 4, *A* and *B*; compare the I_h-induced undershoot during the decay phase of EPSPs; see Berger et al. 2001). Although the majority of the dendritic action potentials was smaller without I_h, they could better summate due to their longer decay (Fig. 4, *A* and *B*). In
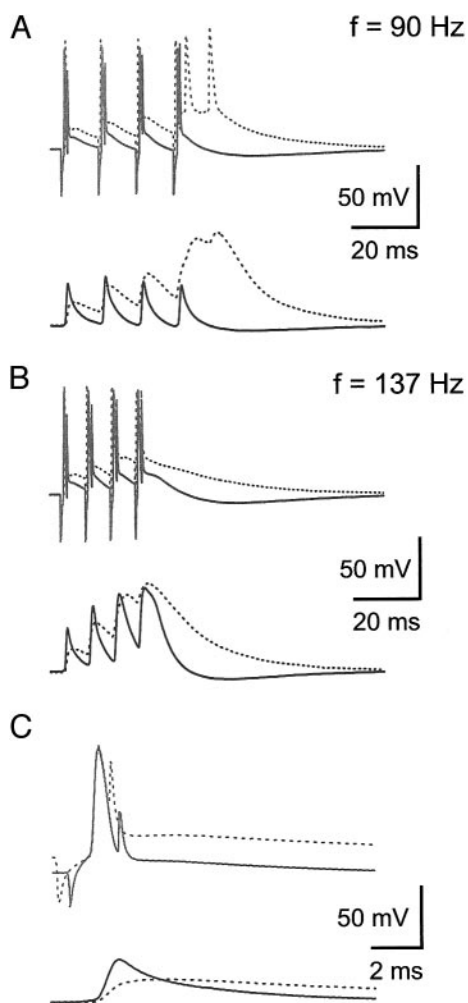
FIG. 4. Blockade of I_h results in a prolongation of the back-propagating dendritic action potential and an increased afterdepolarization of the somatic spike. Using the same experimental paradigm as in Fig. 1, 4 spikes are induced below ($f = 90$ Hz; *A*) and above ($f = 137$ Hz; *B*) the CF. The same protocol is used under control conditions (continuous traces) and under 20 μM ZD7288 (dotted traces). Somatic and dendritic recordings are aligned to the beginning of the 1st spike and are shown superimposed. Under ZD7288, the dendritic action potential becomes smaller and its decay is prolonged. Due to this prolongation, summation is improved and calcium action potentials can be induced. In addition, the afterdepolarization of the somatic spike is markedly increased. *C*: the 1st action potentials from *A* are displayed with an extended time scale showing the kinetic changes in greater detail. *Rat P30,* dendritic recording 280 μm from the soma. Membrane potential under control conditions and under ZD7288 (soma /dendrite): $-68/-64$ mV and $-68/-70$ mV, respectively (depolarizing current was injected to compensate the hyperpolarization due to I_h blockade).

I_h prevents the generation of calcium action potentials with in-vivo-like input

The four-spike-protocol used permitted us to study the relationship between calcium action potential generation in the dendrite and spike frequency in the soma under well-defined conditions. We wanted to further investigate what kind of proximal synaptic activity might activate dendritic calcium spikes under in-vivo-like input conditions. We therefore injected noisy, Gaussian-distributed currents with stationary statistics into the soma, which created the kind of membrane potential deflections seen in vivo. To mimic a realistic population of excitatory and inhibitory presynaptic neurons, we

have chosen a mean $\mu = 200$ or 400 pA, a SD $\sigma = 400$ pA and correlation time constants $\tau = 1\text{--}100$ ms (see METHODS). This resulted in an overall spike frequency of 14.2 ± 2.4 Hz (in 2 cells with 10 realizations of 20 s) and a coefficient of variation of the inter-spike intervals (CV) between 0.5 and 1.72, depending on the correlation time constant τ. Under control conditions, isolated action potentials (no further spike 15 ms before and after the actual one) or doublets were observed in the soma and the dendrite (Fig. 5*A*). Interestingly, calcium action potentials were only rarely seen ($n = 7$ calcium events within the total 200 s of current injection). To investigate the effect of I_h onto the generation of calcium action potentials at similar rates of isolated action potentials, we injected an additional constant somatic current to compensate for the hyperpolarization caused by the blockade of I_h ($\sim$200–300 pA) (see Berger et al. 2001). Blocking I_h with 20 μM ZD7288 markedly increased the number of bursts of somatic action potentials and the concomitant calcium events in the dendrite ($n = 157$ within 200 s of stimulation in 10 realizations; Fig. 5*B*). The average frequency of isolated action potentials was 10.4 Hz, compared with 10.2 Hz under control conditions. The overall action potential frequency including action potentials within bursts was 27.8 ± 10.4 Hz (10 realizations in 2 cells), and the CV increased to values between 0.81 and 2.05 (depending on the correlation
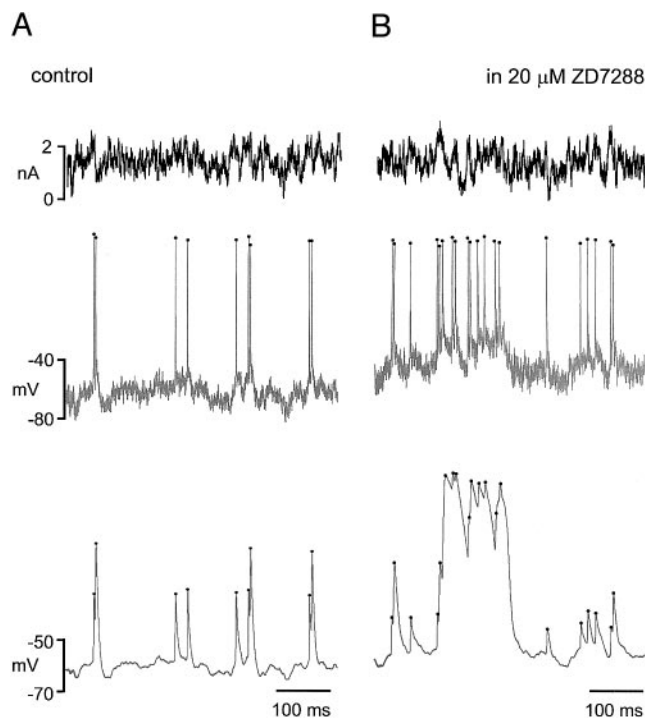

FIG. 5. I_h prevents calcium action potentials under in-vivo-like conditions. Gaussian distributed currents (traces on top) are injected for 20 s into the soma of a pyramidal cell (mean current: 200 pA; sigma: 400 pA; correlation time constant: 3 ms; see METHODS) under control conditions (*A*) and with I_h blocked (*B*). This resulted in noisy membrane potential deflections and irregularly distributed action potentials. *A*: under control conditions, single somatic spikes or pairs of spikes (doublets; *middle traces*) result in the corresponding dendritic action potentials (*bottom traces*). The peaks of the somatic and dendritic action potentials are marked by dots. Calcium action potentials are not seen. *B*: under I_h blockade, bursts of somatic action potentials and the concomitant calcium action potentials in the dendrite are frequently seen. *Rat P37,* dendritic recording 420 μm from the soma. Overall frequency 16.1 Hz under control and 20.9 Hz in 20 μM ZD7288, respectively; coefficient of variation of the inter-spike intervals 0.88 under control and 0.96 in ZD7288, respectively.

time constant τ between 1 and 100 ms). The peak values of the dendritic action potentials were plotted against the inter-spike intervals before the corresponding somatic action potentials (Fig. 6). Under control conditions, the peak depolarizations were all <0 mV, reflecting the absence of dendritic calcium action potentials. Summation of spikes is only seen at brief inter-spike intervals (Fig. 6A). When I_h was blocked, these short inter-spike intervals were sufficient to induce dendritic calcium action potentials. In addition, calcium action potentials were found with much longer somatic inter-spike intervals (Fig. 6B, dotted arrow). These belonged to action potentials generated during a dendritic calcium spike when the preceding inter-spike interval was largely irrelevant.

I_h enhances the critical frequency by impairing the summation properties of back-propagating action potentials

We investigated the effect of I_h on the generation of somatic bursts and dendritic calcium action potentials under in-vivo-like conditions. Only seven calcium action potentials were found under control conditions that were all triggered by a spike triplet in the soma (example shown in Fig. 7A). When blocking I_h, a current with the same statistical properties evoked 157 calcium action potentials. To study the mechanisms of this increased dendritic excitability, we extracted the somatic and dendritic voltage signals around the calcium action potentials (peaks of the dendritic membrane potential beyond –10 mV). The dendritic membrane potentials and the corre-

sponding somatic current injections were aligned at the peak depolarization after the first crossing of the –10-mV threshold and averaged (calcium spike-triggered average; Fig. 7B). Within a time window of 20 ms before the peak, we found an average frequency of 170 Hz (3.4 spikes within the 20 ms preceding the dendritic voltage crossing of –10 mV) under control conditions. The injected somatic current which triggered the calcium spikes reached in the average ~1200 pA immediately before the peak depolarization (Fig. 7B). When I_h was blocked, the dendritic calcium events were longer (Fig. 7C). The calcium spike-triggered average under these conditions revealed a frequency of 140 Hz (2.8 spikes within the 20 ms preceding the dendritic voltage crossing of –10 mV; 82% of control; $P = 0.15$, unpaired t-test; Fig. 7D). The corresponding injected current was smaller (~800 pA) and had its maximum 10 ms before the peak depolarization (Fig. 7D). Hence, under control conditions, only bursts with very high spiking frequency evoked dendritic calcium spikes.

To study the summation of the back-propagating action potential under in-vivo-like conditions, we constructed the sodium spike-triggered average of isolated spikes. As in the four-spike-paradigm, the average back-propagating action potential was narrower and larger in the presence of I_h (Fig. 8A) in comparison to the situation when I_h was blocked (Fig. 8B). The longer dendritic depolarization observed under ZD7288 caused an afterdepolarization in the soma, which in turn increased the probability of triggering subsequent spikes. In
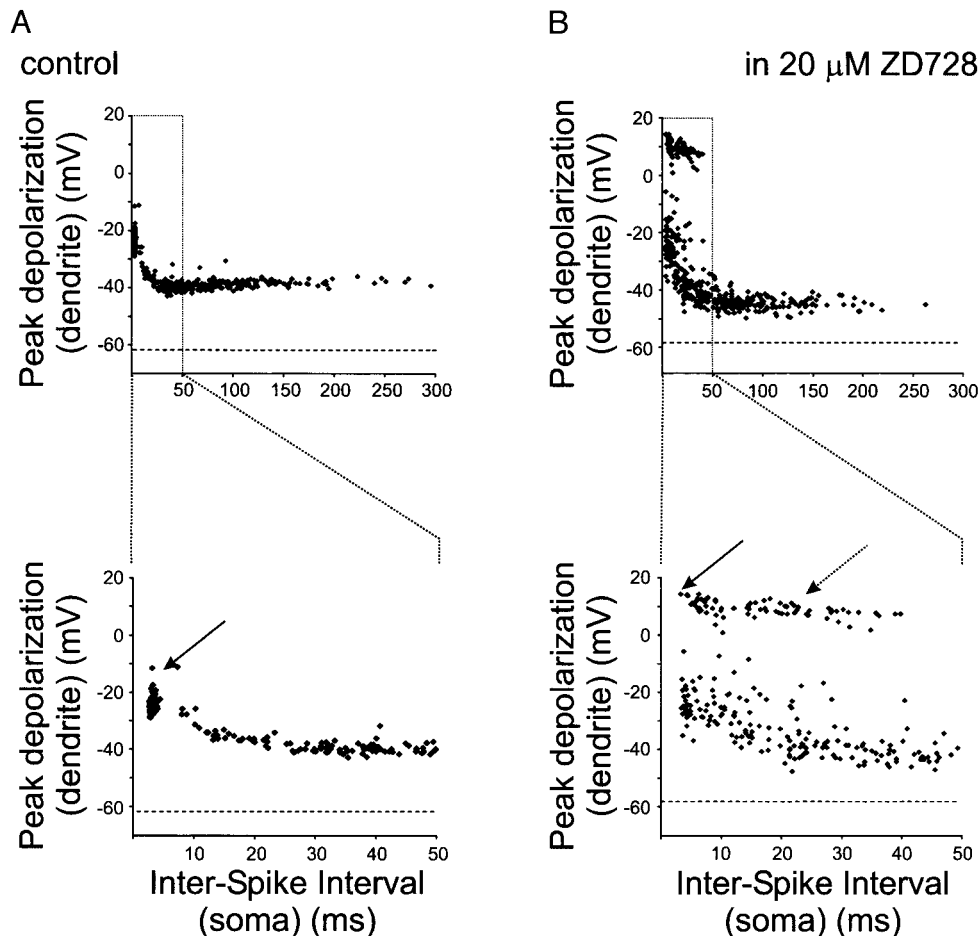

A control

B in 20 μM ZD7288

FIG. 6. I_h prevents calcium action potentials under in-vivo-like conditions. The peak depolarization of the dendritic action potentials is plotted against the inter-spike interval of the corresponding somatic action potential (same realization as in Fig. 5). The data are presented with 2 different scales of the abscissa. A: under control conditions, higher peak depolarizations are observed at brief inter-spike intervals. This reflects the summation of spikes and some additional amplification of the second impulse within a doublet probably due to activation of voltage-gated channels (see arrow). B: the corresponding plots under I_h blockade show now calcium action potentials at comparable inter-spike intervals (see full arrow). In addition, large amplitude calcium action potentials are also found with much longer inter-spike intervals. These are action potentials during a dendritic calcium spike, when the preceding inter-spike interval was largely irrelevant (see dotted arrow). The horizontal line in the plots (–62 mV at control and –58 mV under ZD7288) marks the mean baseline membrane potential during the noisy current injection. The distance from this line to the peak depolarizations given is therefore the actual amplitude of the dendritic spikes.

contrast to the currents necessary to evoke calcium action potentials, there was no difference in the currents necessary to evoke isolated action potentials with and without I_h. To better reveal the effect of I_h, we superimposed the somatic and dendritic action potentials (Fig. 8, *C* and *D*). The average amplitude and decay time constant of the back-propagating action potential was 22 mV and 2.3 ms, respectively, in the presence of I_h, and 10 mV and 7.8 ms when I_h was blocked.

DISCUSSION

I_h increases the electrotonic distance between somatic and dendritic spike initiation zone

Coincident back-propagating somatic action potentials and distal dendritic EPSPs can result in calcium spike firing in the
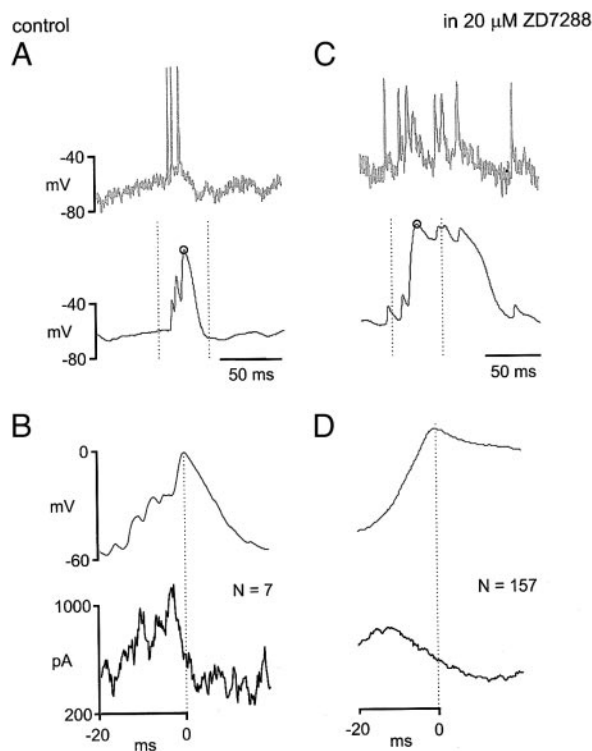
FIG. 7. Generation of dendritic calcium spikes requires a strong synchronized somatic input current. Noisy current is injected under control conditions (*A* and *B*) and with 20 μM ZD7288 (*C* and *D*), respectively. *A*: example of a somatic (*top trace*) and dendritic (*bottom trace*) voltage recording after injection of a Gaussian current ($\mu = 200$ pA, $\sigma = 400$ pA, $\tau = 3$ ms) into the soma. The dendritic calcium action potential (circle on peak) is generated by a somatic spike triplet with a frequency of 120 Hz. Dotted lines show the time interval over which the calcium spike-triggered average in *B* was made. *B*: averaged dendritic voltage traces of the 7 calcium events, which occurred within 100 s of noisy current injection into each of 2 cells (*top trace*; aligned to the 1st peak with an amplitude higher than −10 mV). The corresponding average of the injected current (*bottom trace*) shows that a transient somatic current injection of ≥1,000 pA is required to trigger a dendritic calcium spike under control conditions. *C*: Like *B*, but with I_h blocked. Because the dendritic leak is reduced the calcium-induced dendritic depolarization generates additional somatic spikes, thereby leading to a sustained dendritic depolarization. *D*: averaged dendritic voltage traces of the 157 calcium events occurring within the 100 s of current injection into each of the two cells in the absence of I_h (*top trace*). The average somatic current necessary to trigger a calcium event (lower trace) is much smaller in comparison to control. A calcium event under ZD is preceded by an average spiking frequency of 140 Hz. Note that the corresponding average input current declines ∼10 ms before the peak depolarization is reached. The strong depolarization in the dendrite is due to the evoked calcium current.
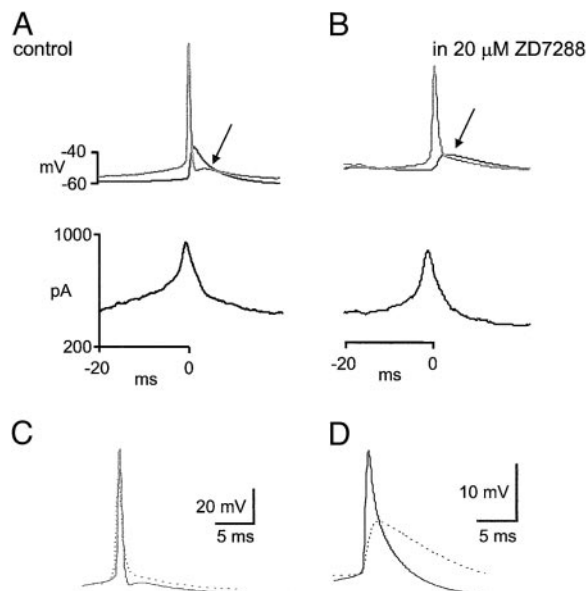
FIG. 8. In the presence of I_h, the dendritic back-propagating action potential is narrow and prevents a somatic afterdepolarization. *A*: action potentials were recorded in the soma and in the dendrite (arrow) and were averaged. Only isolated action potentials were considered (no other spike within 15 ms before and after; in total 2,047 events within twice the 100-s stimulation time; $\mu = 200/400$ pA, $\sigma = 400$ pA). The corresponding averaged current (lower trace) shows that an isolated spike is most effectively triggered by a somatic current transient of ∼1,000 pA. *B*: same as in *A* but with blocked I_h. A total number of 2,069 isolated action potentials were gathered within the same stimulation time (the hyperpolarization due to I_h blockade was compensated by an additional somatic constant current injection). Note that the average back-propagating action potential decays slower than under control conditions (arrow). As a consequence, the somatic action potential shows an afterdepolarization, which enhances the probability of generating an additional spike. *C*: aligning the somatic action potentials with (continuous trace) and without I_h (dotted trace) reveals an additional afterdepolarization of ∼3 mV. *D*: aligning the dendritic action potentials with (continuous trace) and without I_h (dotted trace) shows that I_h increases the amplitude and shortens the decaying phase.

dendrite and bursts of action potentials in the soma (back-propagation-activated calcium spike firing, BAC firing) (Larkum et al. 1999b; Stuart and Häusser 2001). To ensure the associative capability of BAC firing, isolated somatic input alone should not trigger dendritic calcium spikes (but see Larkum and Zhu 2002 for the generation of calcium action potentials by distal input alone). Isolated somatic spikes never trigger dendritic calcium action potentials. Little is known about the underlying mechanism, although it is presumably due in part to the fast repolarization of the action potential due to the I_A conductance as 4-aminopyridine enhances the generation of back-propagating action potential activated calcium spikes (Stuart and Häusser 2001). We studied the generation of dendritic calcium spikes using a train of four spikes initiated by separate current pulses with increasing frequency (Larkum et al. 1999a). When the spikes reach a CF (CF = 104.5 Hz; range: 55.5–166.7 Hz), dendritic calcium action potentials were seen that resulted in enlarged somatic afterdepolarizations. This CF value is identical to that found by Larkum et al. (1999a). In comparison, in vivo recordings in different cortical areas show in general much lower frequencies during tonic firing. Cortical regular spiking cells generated spikes at an overall frequency of 9.4 Hz in the awake state, whereas the spiking frequency increased to 11.8 and 14.0 Hz during slow wave sleep and REM sleep, respectively (nonanesthetized cat) (Steriade et al.

2001). However, under slow wave sleep conditions, a sequence of up and down states was seen with a relatively high firing frequency of ~30 Hz during the up states (Steriade et al. 2001). Studies with anesthetized animals showed a comparable low range of firing rates, but frequency and firing pattern were strongly dependent on the anesthetics used (Paré et al. 1998). In the somatosensory cortex of anesthetized animals even lower overall spiking frequencies were seen ($\leq$10 Hz) (Brecht and Sakmann 2002; Svoboda et al. 1999; Zhu and Connors 1999). These data suggest that calcium action potentials cannot be evoked due to this activity patterns. In contrast to this low tonic activity the firing frequency of layer V pyramidal cells can reach much higher values within bursts (200–400 Hz) (Helmchen et al. 1999; Larkum and Zhu 2002). In the dendrite, so-called complex potentials could be seen in vivo that are presumably the correlate of calcium action potentials found in vitro. These complex potentials occurred spontaneously or were evoked by whisker stimulation (Larkum and Zhu 2002). However, whisker deflection did not always result in a complex potential. Thus a combined distal and proximal input seems to be a prerequisite for this type of activity (compare Larkum et al. 1999b). The presence of bursts was not always accompanied by calcium transients in the distal apical dendrite (Helmchen et al. 1999). In these cases, action potentials with an intra-burst spiking frequency below the critical frequency may have failed to activate the dendritic calcium spike initiation zone.

In another study, action potentials were antidromically evoked in rat pyramidal neurons using spike trains recorded from monkey cortex in vivo as a template (Williams and Stuart 2000b). Here, calcium events dependent on action potential frequency were also recorded in the distal dendrites. Also under these conditions, an instantaneous spike frequency of ~100 Hz was necessary to evoke distal dendritic calcium action potentials. We conclude that in vivo the back-propagating action potentials elicited by proximal synaptic input alone do normally not evoke dendritic calcium spikes. When somatic input is combined with depolarizing current in the dendrite, the CF is decreased as has been shown during BAC firing (Larkum et al. 1999b; Stuart and Häusser 2001).

The hyperpolarization-activated current I_h (Kaupp and Seifert 2001) is a voltage-gated leak conductance. Under steady-state conditions, it causes a depolarizing shift in resting V_m and introduces a persistent shunt. I_h is present at the soma, the basal dendrites, and the apical dendrite in layer V pyramidal cells of the rat somatosensory cortex (Berger et al. 2001; Stuart and Spruston 1998; Williams and Stuart 2000a). However, the I_h channels are unevenly distributed over the somatodendritic compartment with a steep increase in density toward the distal apical dendrite at ~400 μm from the soma (Berger et al. 2001; Lörincz et al. 2002; Williams and Stuart 2000a). The I_h channels in pyramidal cells of the cortex show relatively fast kinetics (activation and deactivation time constants in the range of 10–40 ms) (Berger et al. 2001). This seems to be due to the strong presence of the HCN-1 subunit, which has been shown by in situ hybridization (Mossmang et al. 1999; Santoro et al. 2000), immunocytochemistry (Lörincz et al. 2002; Santoro et al. 1997), and single-cell PCR (Franz et al. 2000). At resting membrane potential only ~5–10% of the channels are open. The uneven distribution of I_h counteracts the morphological influence of the tapering dendrite and equalizes the input

resistance in the distal dendrite and at the soma (Zhu 2000). I_h attenuates synaptic potentials traveling from the soma to the dendrite to a larger extent than those traveling in the opposite direction (Berger et al. 2001). The impact of I_h on the temporal properties of synaptic signals is even stronger: EPSPs are shortened markedly and summation of dendritic inputs is effectively impaired (Berger and Lüscher 2003; Berger et al. 2001; Williams and Stuart 2002).

What is the impact of I_h on dendritic calcium action potential generation due to somatic spike activity? Passive membrane properties of the dendrite increasingly determine the propagation of the action potential the further it progresses into the dendrite. The axial current in front of the action potential encounters a higher membrane resistance and consequently a longer membrane time constant if I_h is blocked. Therefore the dendritic action potential gets slower in rise and decay. Moreover, this slower kinetics may lead to an impaired activation of the remaining dendritic sodium channels and, as a consequence, to a reduction in dendritic action potential amplitude. In a study on the importance of I_h channels for the integrative properties in the dendrites of CA1 pyramidal cells, Magee (1998) found also a shortening of the decaying phase of the dendritic action potential due to I_h. In the present study, we found inhomogeneous effects of I_h blockade on the dendritic action potential amplitude while the decay became always longer. The dendritic spikes appeared more like an EPSP under ZD7288 (compare Berger and Lüscher 2003). Even with decreased dendritic spike amplitudes, the summation was better without I_h and this resulted in a decrease of the CF. In addition to the improvement of the summative properties of the dendrite, longer lasting back-propagating action potentials favor the opening of voltage-gated calcium channels (Markram et al. 1995). Low- and high-voltage-activated calcium channels activate more slowly than sodium channels, and their inactivation time constants are in the range of tens of ms (T-, N-, R- type) or they do not inactivate at all (L-, P-type). Their deactivation, in contrast, is very fast (Magee 1999). A smaller, long depolarization due to a long dendritic spike will therefore be more efficient in the activation of calcium channels in comparison to high-amplitude, short events. Due to the mechanisms discussed in the preceding text, the I_h channels in layer V pyramidal cells with their fast kinetics have opposite effects on burst generation in comparison to I_h channels with slow kinetics like in thalamic relay neurons (time constants in the range of hundreds of ms; based on HCN-2 to -4 subunits) (Franz et al. 2000). These slow I_h channels interact with low-threshold calcium channels and thereby generate rhythmic oscillations of the membrane potential (McCormick and Pape 1990). I_h channels with relatively fast kinetics like in layer V pyramidal cells are in the position to prevent dendritic action potentials and consecutive burst firing.

I_h can be activated by intracellular cAMP, but there are strong differences in the cAMP sensitivity of the different HCN subunits assembling the I_h channels (Kaupp and Seifert 2001). We activated different transmitter systems, to increase the active I_h population and to study its role in the interaction between somatic spikes and dendritic calcium potentials. However, none of the neuromodulatory transmitters (serotonin, isoproterenol, or dopamine) tested over a broad range of concentrations changed the CF. This is possibly due to the presence of I_h channels constituted by HCN subunits with low

cAMP sensitivity (e.g., HCN-1) in the layer V neocortical pyramidal cells. CA1 pyramidal cells lack also an effect of an increased intracellular cAMP level on I_h (Chen et al. 2001). Although layer V and CA1 pyramidal cells possess all four HCN subunits (single-cell PCR) (Franz et al. 2000), the HCN-1 subunit seems to reduce the cAMP sensitivity of the native channels in this cell type. Alternatively, the measurement of the CF may not be sensitive enough to reveal effects of the neuromodulators on I_h channels or the effect of the intracellular cAMP level on other conductances may have covered that one on I_h.

I_h disconnects the two spike initiation zones under in-vivo-like conditions

The CF assessed with the four-spike-paradigm in the presence of I_h is very high, typically ~100 Hz. One may argue that four action potentials at such a high transient frequency are never found in vivo. However, in-vivo-like noisy currents as they may arise from a barrage of asynchronous excitatory and inhibitory synaptic inputs (Shadlen and Newsome 1998) can lead to spike doublets and triplets. If dendritic calcium spikes are meant to represent the binding mechanism between basal and apical input (Larkum et al. 1999b), it would be advantageous that somatic current voltage deflections alone should not be able to evoke dendritic calcium spikes by themselves. In fact, this is what we observed. Only in seven exceptional cases, when somatic spike triplets exceeded a frequency of ~170 Hz, was a calcium spike triggered in the dendrite. The corollary is that, when high-frequency burst are observed in vivo, they are most likely to indicate the simultaneous input to the proximal and distal regions of the cell. The situation changed dramatically when I_h was blocked. Plenty of dendritic calcium spikes ($n = 157$) emerged at a comparable frequency of isolated spikes (~10 Hz). When I_h was blocked, less input current is needed to evoke calcium action potentials. We conclude that I_h efficiently separates the somatic and dendritic initiation zones preventing the proximally located inputs from generating dendritic spikes alone.

Despite the depolarization caused by the noisy current injection, the effect of I_h is not abolished. This is remarkable because a steady depolarization from −65 to −55, for example, would decrease the active population of I_h channels by roughly one half (see Berger et al. 2001). The mechanism by which I_h disconnects the two spike initiation zones is identical to that revealed by the four-spike-paradigm: the presence of I_h reduces the dendritic membrane time constant and shortens the back-propagating action potentials in the dendrite. The shortening of the dendritic action potential has two effects: it diminishes the afterdepolarization of the somatic action potential, thereby reducing the probability for a spike doublet or triplet, and it prevents the summation of the back-propagating action potentials necessary to trigger dendritic calcium spikes.

The slower back-propagating action potential is a direct consequence of the reduced dendritic leak with blocked I_h (Fig. 8D). The concomitant reduction in amplitude, however, cannot be explained by purely passive properties. Because I_h contributes as an additional leak to the total dendritic conductance, $g_D = g_{leak} + g_h$, the dendritic amplitude should increase when this conductance is blocked. This is because in a purely passive model a somatic voltage oscillation with frequency ω appears to be attenuated in the dendrite by a factor $\alpha = 1/\sqrt{(1 + g_D R_T)^2 + (\omega C_D R_T)^2}$, where C_D represents the total dendritic capacitance and R_T the total transfer resistance. The formula confirms that within a passive dendrite a decreased conductance g_D increases the dendritic voltage response evoked by a somatic voltage deflection. The reduced amplitude of the back-propagating action potential observed under blockade of I_h (Figs. 4 and 8D) must therefore be caused by active, voltage-dependent dendritic conductances. A slower rise time of the back-propagating action potential activates less sodium channels because these may inactivate during the slower rising phase. As confirmed by simulations, a slower rise time leads to a markedly reduced amplitude, provided the inactivation time constant of the sodium channels is in the range of the activation time constant (see e.g., Rhodes and Llinás 2001). Active dendritic processes are also revealed by the bi-exponential decay of the back-propagating action potential in the presence of I_h, as opposed to the smaller amplitude and mono-exponential decay without I_h (Fig. 4).

The summation properties of back-propagating action potentials are dominated by the decay phase not the amplitude of the individual dendritic potentials. In fact, the summated dendritic spikes within a high-frequency train may show a smaller peak depolarization in the presence of I_h, despite the fact that the individual amplitudes are larger (Fig. 4). The increased dendritic leak caused by I_h speeds up the dendritic time constant, and this produces a faster and higher back-propagating action potential. Despite the fact that I_h leads to a boosting of the dendritic amplitude, however, it shortens the width and impairs the summation property of the back-propagated action potential. The impaired summation prevents the generation of dendritic calcium spikes by somatic input alone. This mechanism actively disconnects the two spike initiation zones and is therefore an important ingredient for layer V pyramidal neurons to restrict the association properties to joint somatic and distal dendritic input.

REFERENCES

Abeles M. *Corticonics—Neural Circuits of the Cerebral Cortex.* Cambridge, UK: Cambridge Univ. Press, 1991.

Berger T, Larkum ME, and Lüscher H-R. High I_h channel density in the distal apical dendrite of layer V pyramidal cells increases bidirectional attenuation of EPSPs. *J Neurophysiol* 85: 855–868, 2001.

Berger T and Lüscher H-R. Timing and precision of spike initiation in layer V pyramidal cells of the rat somatosensory cortex. *Cereb Cortex* 13: 274–281, 2003.

Brecht M and Sakmann B. Dynamic representation of whisker deflection by synaptic potentials in spiny stellate and pyramidal cells in the barrels and septa of layer 4 rat somatosensory cortex. *J Physiol* 543: 49–70, 2002.

Chen K, Aradi I, Thon N, Eghbal-Ahmadi M, Baram TZ, and Soltesz I. Persistently modified h-channels after complex febrile seizures convert the

seizure-induced enhancement of inhibition to hyperexcitability. *Nat Med* 7: 331–337, 2001.

Cox DR and Miller HD. *The Theory of Stochastic Processes.* London, UK: Methuen, 1965.

Franz O, Liss B, Neu A, and Roeper J. Single-cell mRNA expression of *HCN1* correlates with a fast gating phenotype of hyperpolarization-activated cyclic nucleotide-gated ion channels (I_h) in central neurons. *Eur J Neurosci* 12: 2685–2693, 2000.

Harris NC and Constanti A. Mechanism of block by ZD 7288 of the hyperpolarization-activated inward rectifying current in guinea pig substantia nigra neurons in vitro. *J Neurophysiol* 74: 2366–2378, 1995.

Helmchen F, Svoboda K, Denk W, and Tank DW. In vivo dendritic calcium dynamics in deep-layer cortical pyramidal neurons. *Nat Neurosci* 2: 989–996, 1999.

Kaupp UB and Seifert R. Molecular diversity of pacemaker ion channels. *Annu Rev Physiol* 63: 235–257, 2001.

Larkum ME, Kaiser KMM, and Sakmann B. Calcium electrogenesis in distal apical dendrites of layer 5 pyramidal cells at a critical frequency of back-propagating action potentials. *Proc Natl Acad Sci USA* 96: 14600–14604, 1999a.

Larkum ME and Zhu JJ. Signaling of layer 1 and whisker-evoked Ca^{2+} and Na^+ action potentials in distal and terminal dendrites of rat neocortical pyramidal neurons in vitro and in vivo. *J Neurosci* 22: 6991–7005, 2002.

Larkum ME, Zhu JJ, and Sakmann B. A new cellular mechanism for coupling inputs arriving at different cortical layers. *Nature* 398: 338–341, 1999b.

Lörincz A, Notomi T, Tamas G, Shigemoto R, and Nusser Z. Polarized and compartment-dependent distribution of HCN1 in pyramidal cell dendrites. *Nat Neurosci* 5: 1185–1193, 2002.

Magee JC. Dendritic hyperpolarization-activated currents modify the integrative properties of hippocampal CA1 pyramidal neurons. *J Neurosci* 18: 7613–7624, 1998.

Magee JC. Voltage-gated ion channels in dendrites. In: *Dendrites,* edited by Stuart G, Spruston N, and Häusser M. New York: Oxford, 1999, p. 139–160.

Markram H, Helm PJ, and Sakmann B. Dendritic calcium transients evoked by single back-propagating action potentials in rat neocortical pyramidal neurons. *J Physiol* 485: 1–20, 1995.

McCormick DA and Pape HC. Properties of a hyperpolarization-activated cation current and its role in rhythmic oscillation in thalamic relay neurons. *J Physiol* 431: 291–318, 1990.

Moosmang S, Biel M, Hofmann F, and Ludwig A. Differential distribution of four hyperpolarization-activated cation channels in mouse brain. *Biol Chem* 380: 975–980, 1999.

Pape H-C. Queer current and pacemaker: the hyperpolarization-activated cation current in neurons. *Annu Rev Physiol* 58: 299–327, 1996.

Paré D, Shink E, Gaudreau H, Destexhe A, and Lang EJ. Impact of spontaneous synaptic activity on the resting properties of cat neocortical pyramidal neurons in vivo. *J Neurophysiol* 79: 1450–1460, 1998.

Rhodes PA and Llinás PR. Apical tuft input efficacy in layer 5 pyramidal cells from rat visual cortex. *J Physiol* 536: 167–187, 2001.

Santoro B, Chen S, Lüthi A, Pavlidis P, Shumyatsky GP, Tibbs GR, and Siegelbaum SA. Molecular and functional heterogeneity of hyperpolarization-activated pacemaker channels in the mouse CNS. *J Neurosci* 20: 5264–5275, 2000.

Santoro B, Grant SGN, Bartsch D, and Kandel ER. Interactive cloning with the SH3 domain of N-src identifies a new brain specific ion channel protein, with homology to Eag and cyclic nucleotide channels. *Proc Natl Acad Sci USA* 94: 14815–14820, 1997.

Schiller J, Schiller Y, Stuart G, and Sakmann B. Calcium action potentials restricted to distal apical dendrites of rat neocortical pyramidal neurons. *J Physiol* 505: 605–616, 1997.

Schüz A and Palm G. Density of neurons and synapses in the cerebral cortex of the mouse. *J Comp Neurol* 286: 442–455, 1989.

Shadlen MN and Newsome WT. The variable discharge of cortical neurons: implications for connectivity, computation, and information coding. *J Neurosci* 18: 3870–3896, 1998.

Steriade M, Timofeev I, and Grenier F. Natural waking and sleep states: a view from inside neocortical neurons. *J Neurophysiol* 85: 1969–1985, 2001.

Stuart G and Häusser M. Dendritic coincidence detection of EPSPs and action potentials. *Nat Neurosci* 4: 63–71, 2001.

Stuart G and Sakmann B. Active propagation of somatic action potentials into neocortical pyramidal cell dendrites. *Nature* 367: 69–72, 1994.

Stuart G and Spruston N. Determinants of voltage attenuation in neocortical pyramidal neuron dendrites. *J Neurosci* 18: 3501–3510, 1998.

Svoboda K, Helmchen F, Denk W, and Tank DW. Spread of dendritic excitation in layer 2/3 pyramidal neurons in rat barrel cortex in vivo. *Nat Neurosci* 2: 65–73, 1999.

Tuckwell HC. *Introduction to Theoretical Neurobiology.* Cambridge, UK: Cambridge Univ. Press, 1988.

Williams SR and Stuart GJ. Site independence of EPSP time course is mediated by dendritic I_h in neocortical pyramidal neurons. *J Neurophysiol* 83: 3177–3182, 2000a.

Williams SR and Stuart GJ. Backpropagation of physiological spike trains in neocortical pyramidal neurons: implications for temporal coding in dendrites. *J Neurosci* 15: 8238–8246, 2000b.

Williams SR and Stuart GJ. Dependence of EPSP efficacy on synapse location in neocortical pyramidal neurons. *Science* 295: 1907–1910, 2002.

Zhu JJ. Maturation of layer 5 neocortical pyramidal neurons: amplifying salient layer 1 and layer 4 inputs by Ca^{2+} action potentials in adult rat tuft dendrites. *J Physiol* 526: 571–587, 2000.

Zhu JJ and Connors BW. Intrinsic firing patterns and whisker-evoked synaptic responses of neurons in the rat barrel cortex. *J Neurophysiol* 81: 1171–1183, 1999.